Water Research 233 (2023) 119733

Contents lists available at ScienceDirect

Water Research

journal homepage: www.elsevier.com/locate/watres

Bioremediation of coastal aquaculture effluents spiked with florfenicol using microalgae-based granular sludge – a promising solution for recirculating aquaculture systems

Ana S. Oliveira [a], Marta Alves [a], Frederico Leitão [b,c], Marta Tacão [b], Isabel Henriques [c], Paula M.L. Castro [a], Catarina L. Amorim [a,*]

[a] Universidade Católica Portuguesa, CBQF - Centro de Biotecnologia e Química Fina – Laboratório Associado, Escola Superior de Biotecnologia, Rua Diogo Botelho 1327, Porto 4169-005, Portugal
[b] CESAM and Biology Department, University of Aveiro, Campus Universitário de Santiago, 3810-193 Aveiro, Portugal
[c] Center for Functional Ecology, Department of Life Sciences, Faculty of Sciences and Technology, University of Coimbra, Calçada Martim de Freitas, Coimbra 3000-456, Portugal

ARTICLE INFO

Keywords:
Bioremediation
Florfenicol
Coastal aquaculture effluents
Microalgae-based granular sludge

ABSTRACT

Aquaculture is a crucial industry in the agri-food sector, but it is linked to serious environmental problems. There is a need for efficient treatment systems that allow water recirculation to mitigate pollution and water scarcity. This work aimed to evaluate the self-granulation process of a microalgae-based consortium and its capacity to bioremediate coastal aquaculture streams that sporadically contain the antibiotic florfenicol (FF). A photo-sequencing batch reactor was inoculated with an autochthonous phototrophic microbial consortium and was fed with wastewater mimicking coastal aquaculture streams. A rapid granulation process occurred within ca. 21 days, accompanied by a substantially increase of extracellular polymeric substances in the biomass. The developed microalgae-based granules exhibited high and stable organic carbon removal (83-100%). Sporadically wastewater contained FF which was partially removed (ca. 5.5-11.4%) from the effluent. In periods of FF load, the ammonium removal slightly decreased (from 100 to ca. 70%), recovering 2 days after FF feeding ceased. A high-chemical quality effluent was obtained, complying with ammonium, nitrite, and nitrate concentrations for water recirculation within a coastal aquaculture farm, even during FF feeding periods. Members belonging to the *Chloroidium* genus were predominant in the reactor inoculum (ca. 99%) but were replaced from day-22 onwards by an unidentified microalga from the phylum *Chlorophyta* (>61%). A bacterial community proliferated in the granules after reactor inoculation, whose composition varied in response to feeding conditions. Bacteria from the *Muricauda* and *Filomicrobium* genera, *Rhizobiaceae, Balneolaceae*, and *Parvularculaceae* families, thrived upon FF feeding. This study demonstrates the robustness of microalgae-based granular systems for aquaculture effluent bioremediation, even during periods of FF loading, highlighting their potential as a feasible and compact solution in recirculation aquaculture systems.

1. Introduction

Aquaculture production is strategic in providing food and nutrition and is at a record level, with global production reaching 87.5 million tonnes of aquatic animals in 2020 (FAO, 2022). However, land-based aquacultures require large water volumes to sustain their productivity, generating enormous volumes of effluent carrying suspended solids and pollutants (C, N and P) (Ansari et al., 2019). If not properly handled, these effluents represent a major environmental issue, leading to, among others, the eutrophication of the receiving water bodies (Thomsen et al., 2020). The intensification of fish farming in land-based aquaculture facilities exacerbates the potential negative impacts on surrounding environments due to the concentration of pollutants in limited areas (Li et al., 2021). On the other hand, aquaculture production is highly dependent on some environmental variables (e.g. rainfall, temperature, salinity, etc.) and highly vulnerable to the climate change effects (Ahmed and Turchini, 2021). Therefore, the aquaculture industry has been challenged to maintain its high productivity whilst lowering its

* Corresponding author.
E-mail address: camorim@ucp.pt (C.L. Amorim).

https://doi.org/10.1016/j.watres.2023.119733
Received 28 November 2022; Received in revised form 4 February 2023; Accepted 10 February 2023
Available online 12 February 2023

ecological footprint, to face water scarcity and environmental issues.

Recirculating aquaculture systems (RAS) are highly productive intensive farming systems that make use of technological solutions to effectively treat and recycle aquaculture effluents, reducing the water need and dependence whilst maintaining fish production (Ahmed and Turchini, 2021; Xiao et al., 2019). Nevertheless, to achieve such high standards, successful RAS must ensure a high efficiency of several sequential processes, such as solids removal, dissolved pollutants removal, oxygenation levels and carbon dioxide removal, and lastly, when required, a disinfection step before water recirculation to the fish tanks (Ebeling and Timmons, 2012). While mechanical processes can be easily monitored and controlled, the dissolved pollutants biological removal relies on the interaction of microorganisms, amongst themselves and the incoming wastewater, which greatly influences its efficacy (Schreier et al., 2010).

Although most recent aquaculture practices limit the use of chemicals in fish farming, pharmaceuticals, disinfectants, and antifoulants are still used (Dauda et al., 2019). That is the case of florfenicol (FF), a broad-spectrum antibiotic, which inhibits protein synthesis by binding reversibly to the 50S ribosomal subunit (Zhang et al., 2020). It is broadly used in veterinary medicine, to prevent and treat infectious diseases due to its efficacy, low cost, and high potency (Gao et al., 2018). In fact, since the 1990s, FF has been used in aquaculture farms and currently it is the most used antibiotic, as it is one of the few authorized pharmaceuticals for aquatic medical use (Fernando J. Sutili and Letícia T. Gressler, 2021). A significant antibiotic fraction (70-80%) in its active metabolic form often ends up in the surrounding environment, posing a threat to those ecosystems (Reverter et al., 2020). Indeed, the FF antibiotic has been detected in aquatic systems surrounding fish farms at concentrations ranging between μg L^{-1} to up to mg L^{-1} (Zong et al., 2010). Moreover, the antibiotics present in aquaculture effluents can negatively impact the biological treatment units in RAS, inhibiting organic matter removal, nitrification, and denitrification processes (Gao et al., 2018).

There has been an increasing interest in the use of microalgae for the treatment of saline wastewater, and particularly of aquaculture streams, due to their high adaptability to different salinities, nutrients and contaminants' removal efficiency, lower greenhouse gas emissions, and potential for resource recovery (Lee and Lei, 2019; Li et al., 2019). However, the separation of the biomass from the treated effluent represents a bottleneck in such systems. Microalgae cells' small size (3-30 μm), low density, and negative surface charges, greatly contribute to their poor settling characteristics (Wang et al., 2022). Granulation of microalgae biomass represents an attractive solution to overcome separation and harvesting issues.

Several studies have focused on the use of specific microalgae strains for the treatment of aquaculture effluents in batch assays, many of which aiming at biomass valorization (Ansari et al., 2017; Guldhe et al., 2017; Guo et al., 2013; Khatoon et al., 2016; Liu et al., 2019). Limited studies reported the use of granular biomass, microalgae-bacterial granular sludge and aerobic granular sludge colonized by microalgae, for the bioremediation of such effluents (Fan et al., 2021; Rajitha et al., 2020; Santorio et al., 2022). The present study aims to demonstrate the feasibility to form microalgae-based granules from a native microbial consortium occurring in coastal aquaculture streams in a photo-sequencing reactor, and their efficiency in treating coastal aquaculture effluents. Moreover, the effect of the sporadic presence of FF in wastewater on reactor performance and microbial community were elucidated. It is anticipated that this work would contribute for the application of microalgae-based granules in coastal RAS.

2. Materials and methods

2.1. Microalgae-based granules photo-sequencing reactor set-up

The non-axenic phototrophic microbial consortium used as inoculum was assembled with microbial species obtained from water streams from a coastal aquaculture facility (Riasearch, Portugal). After inoculation, the mixed liquor suspended solids (MLSS) concentration inside the reactor wasof 1.3 g L^{-1}. The column reactor had 2.5 L of working volume, with 110 cm of height and 5.8 cm of internal diameter. Light-emitting diode (LED) light strips (12 V; white color 4000 K; 290 lm m^{-1}) were helically attached to the reactor column and maintained permanently on (24 h of light exposure). The pH was measured but not controlled using a pH sensor EasyFerm Bio Arc 325 (Hamilton) coupled to a Sinope bioreactor controller (Solaris Biotech). Reactor operation was conducted at room temperature (20-31 °C). During the first 21 days, to maximize biomass retention and proliferation inside the reactor and potentiate the granulation process, the reactor was operated with 4-h treatment cycles, as followed: 60 min of feeding introduced at the reactor bottom, during which the reactor was non-aerated; 115 min of aeration with an airflow rate of 3 L min^{-1} and superficial air velocity of 68.2 m h^{-1}; 60 min of settling; and 5 min of effluent withdrawal. Afterwards, 3-h treatment cycles were performed as followed: 60 min of feeding, during which the reactor was non-aerated; a stepwise increase of aeration time from 85 to 112 min; a stepwise decrease of settling time from 30 to 3 min; and 5 min of effluent withdrawal. An automatic timer (Siemens Logo! 230RC) was used to start and stop influent, aeration, and effluent withdrawal. Approximately 35% of the reactor liquid was withdrawn in each cycle.

The reactor operational conditions and wastewater feeding composition, in terms of dissolved organic carbon (DOC), inorganic carbon (IC), phosphate-phosphorous (PO_4^{3-}-P), ammonium-nitrogen (NH_4^+-N), nitrite-nitrogen (NO_2^--N), and nitrate-nitrogen (NO_3^--N), are summarized in Table 1. Acetate was used as a carbon source in the synthetic wastewater. During the three operational phases, the influent wastewater also had 15 g L^{-1} of Red sea salts (Red Sea Aquatics). The wastewater in phases I and II does not mimic typical effluents from coastal aquaculture farms but was used to gradually built-up granules. The wastewater in phase III mimics a real effluent from the coastal aquaculture facility from where the microbial consortium was obtained (Riasearch, Portugal). Four FF shock loads were performed, during which the reactor was fed for 2 consecutive days with wastewater spiked with the antibiotic, at 5 mg L^{-1} (based on the concentration commonly used for bath administrations (Jangaran Nejad et al., 2017)).

2.2. Image analysis

The granulation process was followed through image analysis, using a stereomicroscope (SZ30, Olympus) coupled to a digital camera (C-5060WZ, Olympus). Regularly, biomass samples were collected during the reactor aeration period to ensure the sample representativeness, and multiple images were randomly captured and further analyzed to estimate the granules diameter using automatic tools available in ImageJ software (version 1.53a for MacOS, https://imagej.nih.gov/ij/index.html). At least 340 granules were analyzed in each sampling day. The biomass particles were classified according to their equivalent diameter (Deq) into flocs (0.08 mm $<$ Deq $<$ 0.2 mm), small to intermediate granules (0.02 mm $<$ Deq $\leq$ 1.5 mm), and large granules (Deq $>$ 1.5 mm) (Oliveira et al., 2021, 2020).

2.3. Analytical methods

Wastewater, influent and effluent liquid samples were filtered to remove biomass using 0.45 μm pore size nylon syringe membrane filters (Chromafil® PET filters, Macherey-Nagel). Concentrations of PO_4^{3-}-P, NH_4^+-N, NO_2^--N, and NO_3^--N in the filtrate were determined with photometric test kits (Spectroquant®, Merck Millipore). Concentrations of DOC and IC in the filtrate were determined using a total organic carbon analyzer (TOC-V CSH/CSN, Shimadzu), according to the combustion-infrared method.

Quantification of the FF content in the filtrate was performed using high-performance liquid chromatography (HPLC) on a Pump-126

Table 1
Reactor operational conditions and wastewater composition throughout operation.

Phase	Duration (operational days)	HRT (h) [a]	Concentration (mg L^{-1})					
			DOC	IC	PO_4^{3-}-P	NH_4^+-N	NO_2^--N	NO_3^--N
I	21 (day-0 to -21)	10.5	139	12	9.2	15.4	-	-
II	21 (day-22 to -43)	7.9	55	17	7.3	2.7	0.13	4
III	144 (day-44 to -188)	7.9	26	26	5.1	0.3	0.25	8
	8 days ([b])	7.9	28	26				

[a] Hydraulic retention time
[b] Four FF shock loads were applied during phase III for 2 consecutive days on day-133 to -135, day-139 to -141, day-167 to -169, and day-181 to -183

Solvent module System Gold (Beckman Coulter) with a LiChroCART 250-4 LiChrospher 100 RP-18 reversed-phase column, 5 mm particle size (Merck), and using a Autosampler Prostar 410 (Varian). Mobile phase consisted of 40/60% (v/v) acetonitrile/water acidified with trifluoro-acetic acid (pH 2.0); flow rate of 0.8 mL min^{-1}; running time of 8 min (FF elution time ca. 5.3 min). Compound detection was performed with a fluorescence detector Prostar 363 (Varian), excitation and emission wavelengths corresponded to 230 and 284 nm, respectively. Fluorine ions concentration in the filtrate was determined as described by Duque et al. (2011).

The microalgae-based granular sludge bed-height was determined after the settling time using a graduated scale placed on the reactor column. Total suspended solids (TSS), volatile suspended solids (VSS), MLSS, and mixed liquor volatile suspended solids (MLVSS) were analyzed in accordance with standard methods (APHA, 1998).

Dissolved oxygen level was measured using a Dual input meter HQ40D with a dissolved oxygen probe LDO101 (Hach) during 3 treatment cycles without FF and 3 treatment cycles with FF in the wastewater.

2.4. FF photodegradation

To ascertain on the contribution of the photodegradation process for the FF removal, a control reactor without biomass was setup as described in section 2.1, and filled with 2.5 L of a medium with the same composition as the reactor influent after feeding: 4.90 mg L^{-1} PO_4^{3-}-P, 0.04 mg L^{-1} NH_4^+-N, 2.40 mg L^{-1} NO_2^--N, 5.0 mg L^{-1} NO_3^--N, 8.9 mg L^{-1} DOC, 28 mg L^{-1} IC, 5.88 mg L^{-1} FF, 15 g L^{-1} Red sea salts (Red Sea Aquatics). The reactor was operated mimicking a 3-h treatment cycle (as described in section 2.1) and liquid samples were collected at the beginning of the cycle, and beginning and end of aeration to determine the FF concentration. A total of three treatment cycles were performed.

2.5. Extraction and quantification of chlorophyll a, b and total carotenoids

The reactor biomass was collected during the aeration period and crushed using a pottering tube and a pestle. Chlorophyll a and b and total carotenoids were extracted from the biomass using methanol as an organic solvent, without any cell wall disruption method (Henriques et al., 2007). The absorbance was determined at 665, 652 and 470 nm wavelengths using a spectrophotometer Thermo Spectronic Helios Gamma 9423 UVG 1000E UV-VIS. Concentrations of chlorophyll a, b and total carotenoids were calculated using the equations established for the methanol pigments' extraction method (Sumanta et al., 2014).

2.6. EPS extraction and characterization

The EPS extraction was performed in triplicate (n=3) using 0.5% (w/v) of sodium carbonate, heat (80°C) and magnetic stirring (400 rpm) for 35 min. Afterwards, the mixture was centrifuged at 4000 × g and 4 °C for 20 min, the pellet was discarded, and the supernatant was stored at -20 °C. Colorimetric methods were used to access the EPS content in polysaccharides (Dubois et al., 1956) and proteins (Lowry et al., 1951).

2.7. DNA extraction and next generation sequencing (NGS)

Biomass was collected and crushed under aseptic conditions (section 2.5). The resulting suspension was used for DNA extraction using the DNeasy Power Soil kit (Qiagen).

The variable regions V5-V7 of the 16S rRNA gene and V8-V9 of the 18S rRNA gene were sequenced on the Illumina MiSeq platform (Eurofins Genomics), applying 2×300 bp paired-end read libraries and using the following primers set: (799F2 (5'- AACMGGATTAGATACCCGG- 3')/ 1193R (5'- ACGTCATCCCCACCTTCC - 3') (Bodenhausen et al., 2013; Bulgarelli et al., 2012), and V8F (5'- ATAACAGGTCTGTGATGCCCT - 3') /1510R (5'- CCTTCYGCAGGTTCACCTAC - 3') (Amaral-Zettler et al., 2009; Bradley et al., 2016), respectively.

The raw paired-end reads were demultiplexed, assembled and analyzed using QIIME2 (v2021.4) (Bolyen et al., 2019), to identify ASVs (Amplicon Sequence Variants). DADA2 was used for denoising, chimera removal and trimming (Callahan et al., 2016). Microbial taxonomy was assigned using a naive Bayes classifier trained on the SILVA 132 99% database (silva-132-99-nb-classifer) (Quast et al., 2013). Singleton ASVs were removed. For 16S rRNA gene datasets ASVs identified as eukaryotes, mitochondria or chloroplasts, were removed. Inversely, prokaryotes were removed from 18S rRNA gene datasets.

The biomass samples' raw sequenced data was deposited in the Sequence Read Archive from NCBI database, BioProject accession number: PRJNA922107.

2.8. Statistical analysis

A one-way ANOVA and subsequent post-hoc Tukey comparison, with $p<0.05$ established for significance, were carried out to investigate differences in each EPS component concentration and the protein-to-polysaccharide ratio (PN/PS ratio), using the SPSS program (SPSS Inc., Chicago, IL Version 26.0). Normal distribution was verified with the Shapiro-Wilk test ($p>0.05$).

Microbiome comparisons and diversity were analyzed using MicrobiomeAnalyst (Dhariwal et al., 2017). Alpha diversity was calculated using Richness (total number of observed ASVs), Shannon (Shannon--Wiener- *H'*) and Evenness (Pielou's evenness index – *J'*) indexes. Beta diversity metrics were visualized using Non-metric MultiDimensional Scaling (NMDS) graphics based on Bray–Curtis dissimilarity index, and verified using a nonparametric PERMANOVA test with 999 permutations, followed by a Monte-Carlo test, using Permanova+ (V 1.0.3) for Primer 6 (V 6.1.13) (Anderson et al., 2008). A $p<0.05$ was considered significant. Univariate Statistical Comparisons package included in MicrobiomeAnalyst was used at feature-level using t-test with a *p*-value cutoff adjusted to 0.05.

3. Results

3.1. Development of microalgae-based granular sludge and its characteristics

3.1.1. Granules' morphology

The seed biomass was mainly composed by flocs with a loose

structure. After 21 days, irregularly shaped granules started to appear, with floccular and filamentous structures still being observed (Fig. 1). These biomass structural changes were accompanied by an increase of the biomass settling velocity, from 0.933 to 9.33m h^{-1} during the first 21 days. From day-41 onwards, round regular-shaped granules dominated the biomass (Fig. 1). A transition in the aggregate's coloration from light to dark green was also observed.

The size distribution of biomass particles and granules was monitored regularly (Fig. 2) and classified according to their equivalent diameter (Deq) into flocs (0.08 mm < Deq < 0.2 mm), small to intermediate granules (0.2 mm < Deq ≤ 1.5 mm), and large granules (Deq > 1.5 mm). During phase I, minor changes were observed in the floc's percentage (53 to 51%) and in small to intermediate granules (47 to 49%), while large granules were present in a neglectable number. The high percentage of small to intermediate granules on day-0 occurred because the microbial consortium used as inoculum tended to aggregate or form large flocs of filamentous biomass during its cultivation prior to reactor inoculation. Nevertheless, the biomass clearly shows an evolution towards granulation between day-0 and -21, showing less flocs with a loose structure (Fig. 1). From day-41 onwards, small to intermediate granules became predominant in the biomass, and the number of large granules increased gradually, reaching up to 27% of the biomass on day-146. Flocs numbers increased again towards the end of reactor operation as biomass showed a more even distribution between the three established Deq ranges.

During phase I, as the granulation process occurred, the effluent TSS and VSS contents (exhibiting identical values) gradually decreased from 0.4 ± 0.01 to 0.02 ± 0.001 g L^{-1}, stabilizing thereafter within a low range of 0.006-0.037 g L^{-1} (Fig. S1). On the other hand, till day-85, the MLSS and MLVSS concentrations in the reactor increased from 1.3 to 9.1 g L^{-1} and 1.1 to 7.6 g L^{-1}, stabilizing thereafter even during FF shock loads with average concentrations of 5.5 ± 1.1 g L^{-1} and 4.4 ± 0.9 g L^{-1}, respectively (Table S1). In fact, during phase III, when mature granules were well established in the reactor, the biomass bed-height exhibited overall low values, ranging between 3 and 5.75 cm but the sporadic presence of FF in the wastewater did not cause major disturbances neither in the effluent's solids contents nor in the bed-height (Fig. S1).

3.1.2. Dynamics of the EPS content in biomass

Throughout operation, the EPS composition within the granules differed significantly in terms of polysaccharides, proteins, and PN/PS ratio ($p<0.05$) (Fig. 3). The main EPS component varied throughout operation, as polysaccharides' concentration surpassed that of proteins on some days (day-0, -64, -85, -126, -167, and -188), and the opposite occurred on the remaining analyzed days (day-22, -41, -105, and -147). The EPS polysaccharides' content increased gradually from day-0 to -64, followed by a sharp increase on day-85 reaching a maximum concentration of 110 ± 32 mg g^{-1} TSS. Afterwards, polysaccharides concentrations decreased significantly until day-147 ($p<0.05$), increasing again towards the end of reactor operation (day-167 and -188). A sharp increase of the EPS proteins' content was observed from day-0 to -22, 0.8 ± 0.05 to 38.5 ± 2.6 mg g^{-1} TSS, contributing to the drastic rise of PN/PS ratio (0.1 ± 0.01 to 2.0 ± 0.17). The maximum proteins concentration in the EPS was detected on day-85, ca. 70 ± 21 mg g^{-1} TSS, after which only minor variations occurred without significant differences ($p>0.05$), even in periods when FF was present in the wastewater. Despite the maximum concentrations of polysaccharides and proteins being reached on day-85, polysaccharides' content had a higher contribution for total EPS on that day, leading to the lowest mean PN/PS ratio of phase III (0.6 ± 0.01). After day-85, the EPS exhibited significant fluctuations in the PN/PS ratio ($p<0.05$).

3.1.3. Dynamics of the pigments content in biomass

A pronounced increase of chlorophyll a, b and total carotenoids contents in the biomass was observed from day-0 to -64, reaching ca. 1546 ± 63 μg mg^{-1} TS of total pigments (sum of chlorophyll a and b and carotenoids) representing a 23-fold increase (Fig. 4). From day-85 onwards, the pigments content stabilized, even in periods when FF was present in the wastewater. Throughout operation, chlorophyll a was the predominant pigment produced by the biomass, followed by carotenoids and chlorophyll b.

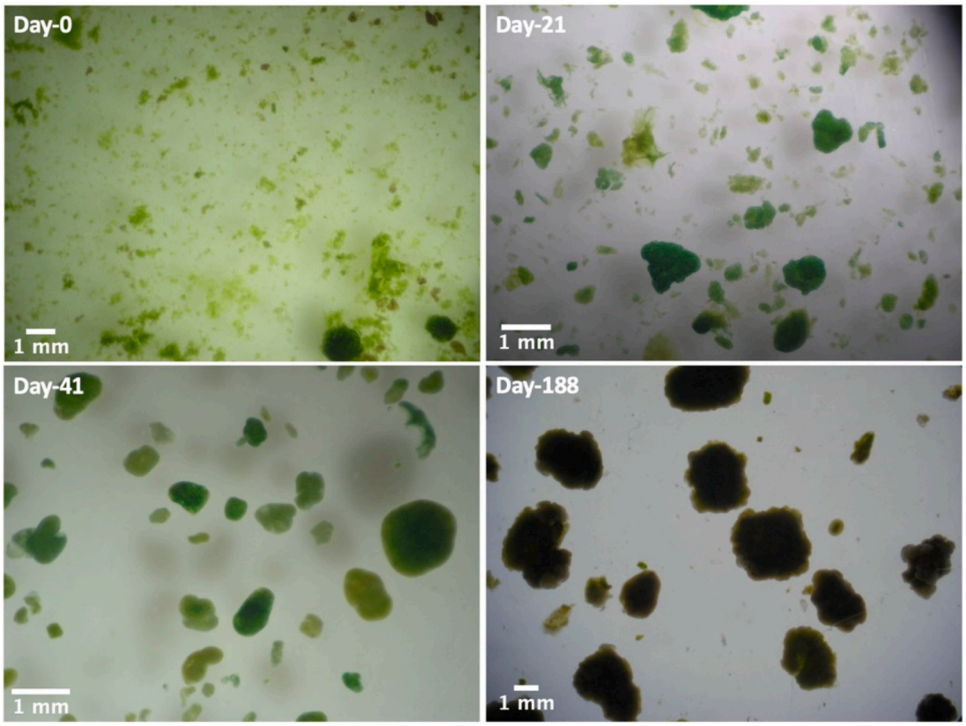

Fig. 1. Microalgae-based biomass morphology in different reactor operational days: day-0 (inoculum), day-21 (phase I), day-41 (phase II), and day-188 (phase III).

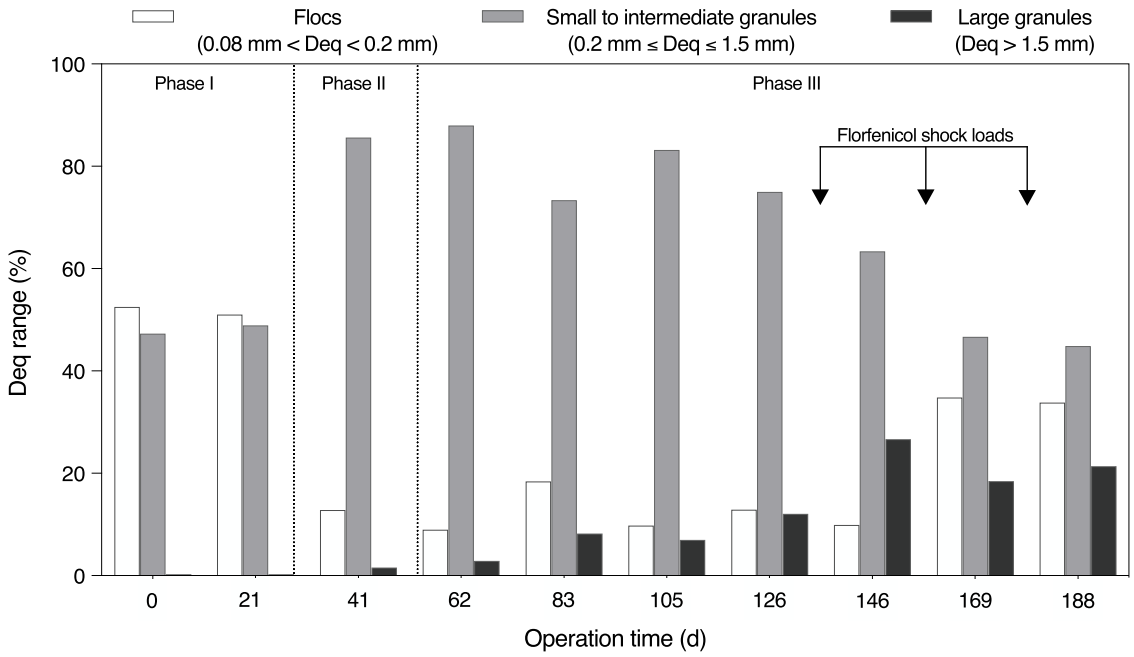

Fig. 2. Microalgae-based granule's size distribution over reactor operation. Arrows mark the FF shock loads.

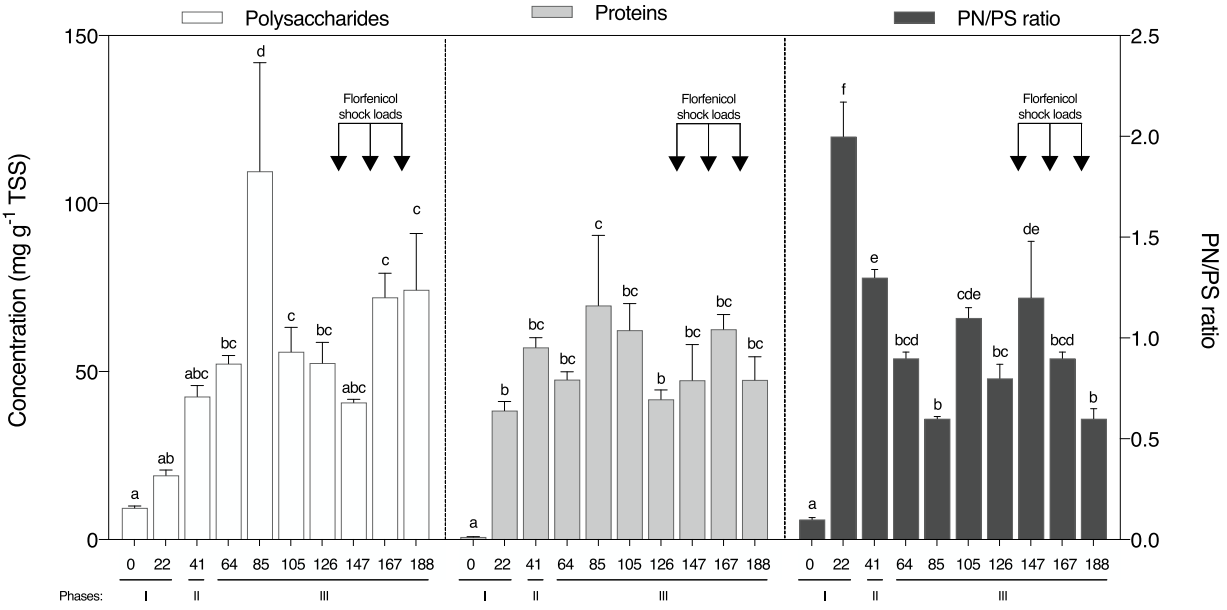

Fig. 3. Concentrations (mg g^{-1} TSS) of polysaccharides and proteins, and the protein-to-polysaccharide ratio (PN/PS) of EPS. Columns represent the mean of triplicates (n=3) and error bars represent the standard deviation. Means that do not share a letter in columns of the same group differed significantly according to Tukey's test at $p<0.05$. Arrows mark the FF shock loads.

3.2. Reactor performance and effluent quality

3.2.1. Carbon removal

High DOC removal efficiencies were achieved shortly after the beginning of operation, with an average removal of 89 ± 21 % and 94 ± 6 % during phases I and II, respectively (Fig. 5a). As the DOC in the wastewater decreased in phase III, the system maintained its high removal efficiency with minor variations, namely during the FF shock loads, during which removal efficiencies ranged between 83 and 100%.

3.2.2. N species and phosphate removal

The ammonium removal efficiency (Fig. 5b) during phases I, II and early phase III fluctuated greatly (6 to 94%). Complete ammonium removal was achieved around day-70 (phase III), with small variations in the removal efficiency occurring whenever FF was absent from the wastewater, maintaining an ammonium depletion efficiency of ca. 93-100%. During the four periods when the antibiotic FF was present in the wastewater, a decline of the ammonium removal efficiency occurred to 74, 78, 74 and 70%, respectively, being reestablished 2 days after the FF feeding ceased.

Nitrate was introduced into the feeding wastewater in phases II and III of reactor operation (Fig. 5c). The nitrate removal increased considerably during phase II, reaching its maximum efficiency (ca. 75%). Subsequently, in phase III, nitrate removal fluctuated greatly before and during FF shock loads (13-73%).

Similarly to nitrate, nitrite was integrated into the wastewater from

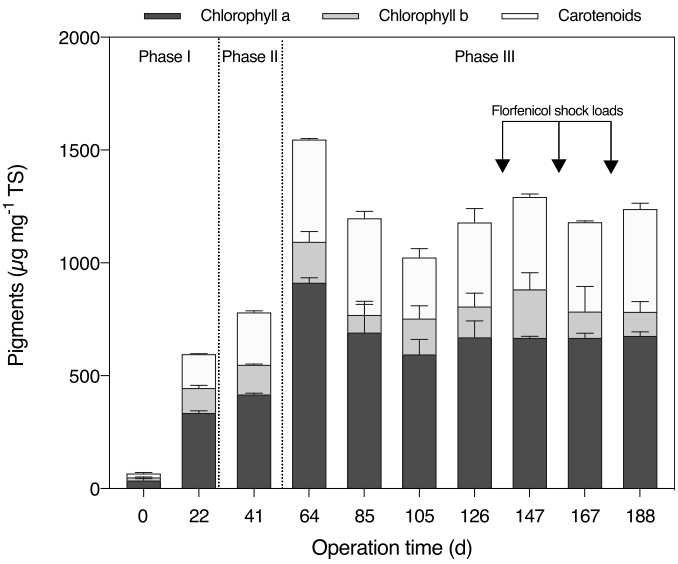

Fig. 4. Concentrations (μg mg^{-1} TS) of chlorophyll a and b and carotenoids in the biomass along reactor operation. Columns represent the mean of duplicates (n=2) and error bars the standard deviation. Arrows mark the FF shock loads.

phase II onwards (Fig. 5d). On most days, a slight nitrite consumption occurred during the aerobic period of the treatment cycle. However, this removal was not sufficiently expressive, leading to higher nitrite levels in the effluent than those in the feeding and to the accumulation of this nitrogen form in the reactor.

The overall N removal ranged between 93 and 94% during phase I, 18 and 79% during phase II, and 4 and 62% during phase III, with the lowest removal being achieved during a FF shock.

Phosphate removal efficiency fluctuated during operation, showing low overall removal of this compound and a maximum efficiency of 46% around day-49 (Fig. 5e).

3.2.3. Dissolved oxygen and pH in the effluent

Minimum dissolved oxygen concentrations in the reactor bulk liquid were reached during the feeding period of the treatment cycle, during which the reactor was non-aerated. Also, the antibiotic presence in the wastewater contributed to a slight increase in dissolved oxygen levels, as a minimum of 7.4 ± 0.4 mg O_2 L^{-1} in the absence of FF and 8.4 ± 0.4 mg O_2 L^{-1} in the presence of FF were detected (Fig. S2).

In phases I, II and III, the pH values during the operational cycles ranged from 7.6 to 8.8, 8.2 to 8.5, and 8.4 to 9.2, respectively, stabilizing in the last phase. Whenever the wastewater contained FF, no relevant pH variations were detected (Fig. S3).

3.3.4. Fate of FF

During phase III, the reactor biomass was exposed to the intermittent presence of FF in the wastewater for four periods of two consecutive days. Table 2 shows the mass balance of FF in the reactor. The FF removal in each shock load of the antibiotic was low. Based on the FF deficit observed between its concentration in the wastewater and in the effluent, microalgae-based granules removed ca. 11.4, 7.9 and 5.3 mg of FF in the first, third and fourth shocks, respectively. On the other hand, FF was released on the second shock given the higher FF content in the effluent (87.1 mg) than in the wastewater (79.8 mg). On the HPLC profiles of the effluent samples, no metabolites resulting from FF degradation were detected (Fig. S4). Furthermore, fluorine ions content in the effluent samples was negligible (Fig. S5). Removal of FF due to photodegradation was tested, since the presence of nitrate and dissolved organic matter in the medium can affect the FF photolysis, and showed to be negligible as the antibiotic was not susceptible to photodegradation within the treatment cycles established (Fig. S6).

3.4. Evolution of the microbial communities in biomass

3.4.1. Microalgae community

A total number of 802871 reads were obtained from 10 samples, with the vast majority of the ASVs (85%) affiliated with taxonomic groups other than microalgae. Microalgae were represented by 13 ASVs (712349 reads), distributed over 4 different phyla (*Chlorophyta, Charophyta, Bacillariophyta*, and *Ochrophyta*).

The microalgae community exhibited low diversity (Shannon index between 0.02 and 0.724), richness (4 to 10 ASVs per sample), and equitability (0.014 to 0.372) (Fig. S7). The genus *Chloroidium* was predominant in the inoculum (ca. 99%), but its abundance gradually decreased over time, reaching a relative abundance lower than 0.1% from day-105 onwards. Concomitantly, an unidentified microalgae species from the *Chlorophyta* phylum, not detected in the inoculum, was the most abundant taxa from day-22 onwards (>61%). Also, an ASV assigned to the genus *Nitzschia* was first identified in the biomass on day-167 and its abundance increased towards the end of operation, reaching ca. 13% on day-188.

3.4.2. Bacterial community

Ten samples were sequenced, but on day-0 no reads were obtained. A total number of 70124 reads was obtained from the remaining 9 samples, corresponding to 126 ASVs assigned to 8 different bacterial phyla.

The community diversity (Shannon index) increased gradually until day-126 (Fig. 6a). The presence of FF in the wastewater triggered a decrease of the bacterial diversity, showing values ca. 13% lower than those on day-126, prior to the first FF shock load. The community evenness, on the other hand, showed a general decrease throughout operation, with abrupt reductions upon the feeding with wastewater mimicking coastal aquaculture effluents (phase III) and upon the load of wastewater containing FF. The NMDS ordination plot (Fig. 6b) revealed noticeable changes in the bacterial community structure over time, with the distribution of the samples in the plot reflecting the sampling timeline. In the later sampling times, a greater stability of the communities is noted, reflected in a tight clustering between samples from day-147, -167 and -188.

Pseudomonadota was the most abundant phylum in all samples, representing on average 59.5 ± 8.8%, followed by *Bacteroidota* (23.2 ± 11.9%), and *Planctomycetota* (16.6 ± 6.9%). These three phyla were present in all samples (Fig. S8).

At genus level, *Marinobacter, Roseovarius, Pseudomonas*, an unknown *Phycisphaeraceae* member (SM1A02), and an uncultured genus assigned to the *Saprospiraceae* family were present in all samples collected from day-22 to -188, representing together 29.8 to 77.8% of the total bacterial community (Fig. 7a). Despite not being detected in all samples, members from the *Thauera, Muricauda*, and *Sphingorhabdus* genera, represented a large portion of the bacterial community as well, particularly in phase III. Members of the *Thauera* and *Muricauda* genera were detected from day-41 and -105 onwards, reaching 17.5 and 27.0% of the total community on day-188, respectively. The *Sphingorhabdus* taxon first observed on day-64, increased its abundance to 10.1% of the total community on day-105. Together, these three genera reached a maximum relative abundance of 45.8% on day-188.

During phase III, the wastewater composition along with the sporadic presence of FF in the wastewater changed the bacterial community taxonomic composition (Fig. 7b). Upon the introduction of a feeding medium that mimics a coastal aquaculture effluent, the relative abundance of several genera increased, as it is the case of *Roseovarius, Muricauda, Thaurea, Sphingorhabdus*, and *Paracoccus*, which relative abundance by the end of operation increased from 1.3 to 21.7%, 0 to 11.4%, 2.2 to 9.9%, 0 to 5.6, and 0 to 0.3%, respectively. For other community members, the opposite occurred, with their abundance decreasing considerably, namely: *Pseudomonas* (15.6 to 0 %), *Marinobacter* (6.5 to 0.6%), and *Stappia* (1.8 to 0%) (Fig. S9). The relative abundance of genera *Roseovarius, Muricauda*, and *Filomicrobium*

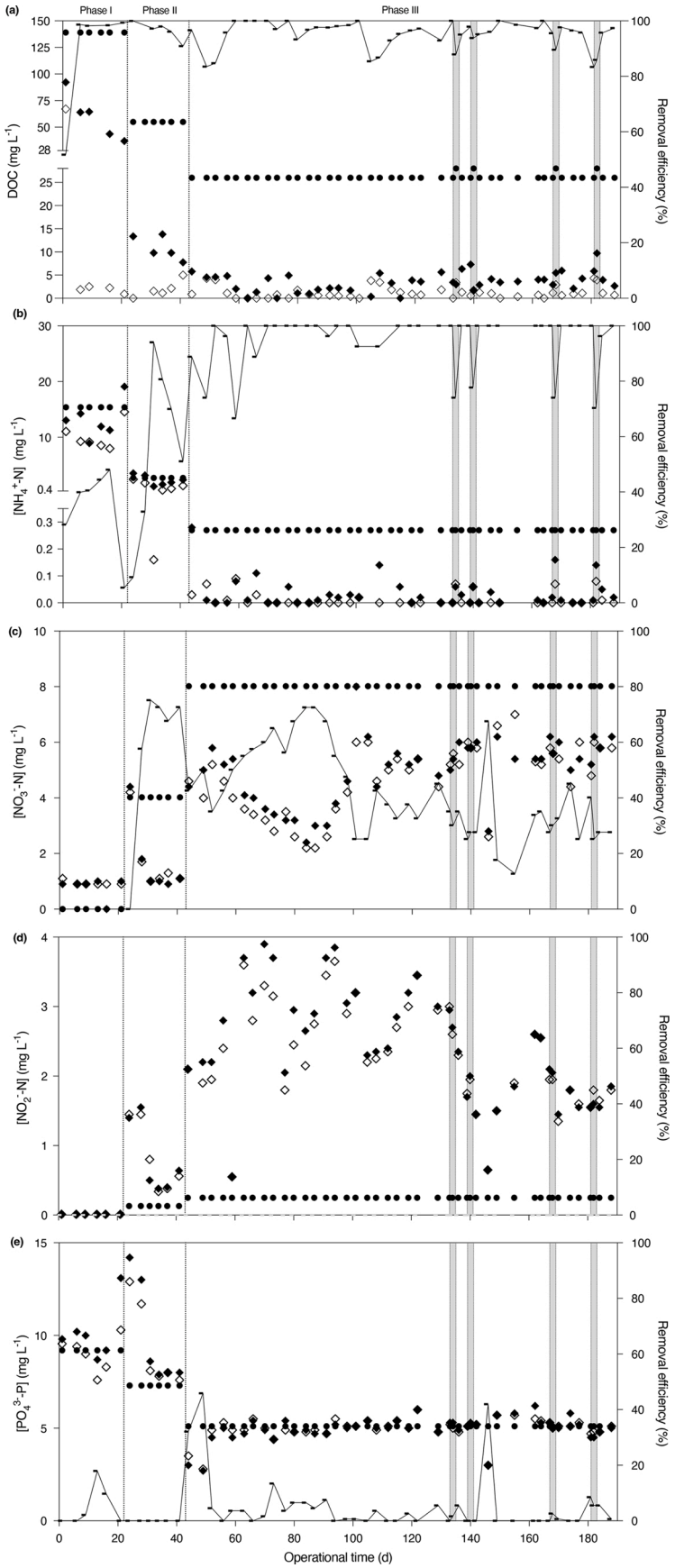

Fig. 5. Concentration (mg L^{-1}) of DOC (a), NH_4^+-N (b), NO_3^--N (c), NO_2^--N (d), and PO_4^{3-}-P (e) in the wastewater (●), influent after feeding (◆), and effluent (◊), and the respective removal efficiencies (-). Gray bars indicate the periods of FF loading shocks.

Table 2
Mass balance of FF in the reactor during the four shock loads.

FF shock load	FF mass balance (mg)		
	FF in the wastewater	FF in the effluent	FF removed *
1st	97.9	86.5	11.4
2nd	79.8	87.1	n.d.
3rd	94.2	86.2	7.9
4th	105.8	100.5	5.5
Total in the four shock loads	377.7	360.2	17.4

* Estimated based on the FF concentrations in the wastewater and effluent. n.d.: not detected

increased from 21.7 to 29.3%, 11.4 to 22%, and 2.8 to 4.6%, respectively, after the first FF shock load. Contrarily, the relative abundances of unknown genus *SM1A02* of the *Phycisphaeraceae* family, uncultured genus assigned to the *Saprospiraceae* family, *Ruegeria, Sphingorhabdus*, and *Paracocccus* decreased during the same period from 18.3 to 13%, 0.6 to 0.2%, 4.2 to 0.4%, 5.6 to 2.8%, and 0.3 to 0%, respectively (Fig. S9). Statistical analysis (t-test, $p<0.05$) revealed that eleven ASVs showed significantly different relative abundances before and after the FF shock loadings within phase III. In fact, the relative abundance of five ASVs decreased - ASVs assigned to genera *Hyphomonas* and *Thauera*, families *Rhizobiaceae* and *Saprospiraceae*, and order *Parvibaculales* - whilst the remaining ASVs increased their relative abundancies - ASVs assigned to genera *Muricauda* and *Filomicrobium*, and families *Balneolaceae, Rhizobiaceae*, and *Parvularculaceae* (Fig. 8).

4. Discussion

A microalgae-based granular sludge was developed in a photosequencing reactor and successfully applied to remove carbon and nutrients from coastal aquaculture effluents, even when the antibiotic FF was present in those effluents. The chemical quality of the treated water would allow recirculation of water back into the fish tanks, representing a potential alternative biological treatment system that can be implemented as part of a RAS.

The phototrophic microbial consortium autochthonous to the water streams of a coastal aquaculture facility successfully self-granulated within 21 days, without the need of any carrier material (Fig. 1). After those 21 days, small to intermediate granules (0.2 mm < Deq ≤ 1.5 mm) were the predominant biomass form in the reactor. Nevertheless, towards the end of operation (day-169 to -188) the abundance of small to intermediate granules and large granules decreased, and the abundance of flocs increased (Fig. 2). The upsurge of flocs is often associated with the breakage of large and intermediate granules into smaller granules and fragments (Oliveira et al., 2021, 2020), which may be due to the long operational period and/or environmental stressors (e.g., the antibiotic FF).

Stable and low biomass bed-height and effluents' solid (TSS and VSS) contents were detected throughout operation. A similar trend was reported by Santorio et al. (2021) that used an aerobic granular sludge system to treat freshwater aquaculture effluents. The low carbon and nitrogen concentrations in this kind of effluents induce a metabolic selective pressure, only supporting the viability of small biomass portions. This low biomass content (5.1 ± 2.2 g $_{MLSS}$ L^{-1}, Table S1) was indeed sufficient to ensure the efficient treatment of the coastal aquaculture wastewater, achieving high removal efficiencies, crucial for water recirculation.

Microalgae pigments are indirect biomarkers of cell viability. Furthermore, microalgae demonstrate their adaptation to various stimuli through changes in enzymes, hydrocarbon, and pigment levels (Vo et al., 2020). In the present study, pigments concentrations increased sharply until day-65, stabilizing thereafter even in periods when wastewater contained FF (Fig. 4). These results, as well as the granules' coloration shift from light to dark green, are likely due to an initial microalgae proliferation and subsequent adaptation to the feeding composition, granulation process, and dynamics of the bacterial community co-habiting the granules.

The EPS production increase in the first days of operation is linked to the granulation process and to the biomass higher settleability. Moreover, as pointed out in previous studies, a higher relative hydrophobicity is linked to a higher PN/PS ratio, which in turn is considered a triggering factor for granulation (Wang et al., 2022). Indeed, a PN/PS ratio sharp increase occurred from day-0 to -22, pointing this period as the beginning of the granulation process (Fig. 3). The EPS biosynthesis is an intensive energy- and resource-consuming process, inevitably affecting microbial growth and competitiveness of EPS producers (An et al., 2016). A high loaded wastewater was used at the beginning of operation, so that microorganisms have enough energy to proliferate and produce EPS, which could benefit the self-aggregation process. The stepwise carbon decrease in the feeding could have contributed for the granule's formation and stabilization in the early stages of operation. Perhaps a start-up period to acclimatize the biomass to the operating and feeding conditions is not needed. Nevertheless, further research with low DOC in the start-up wastewater is needed to confirm this hypothesis.

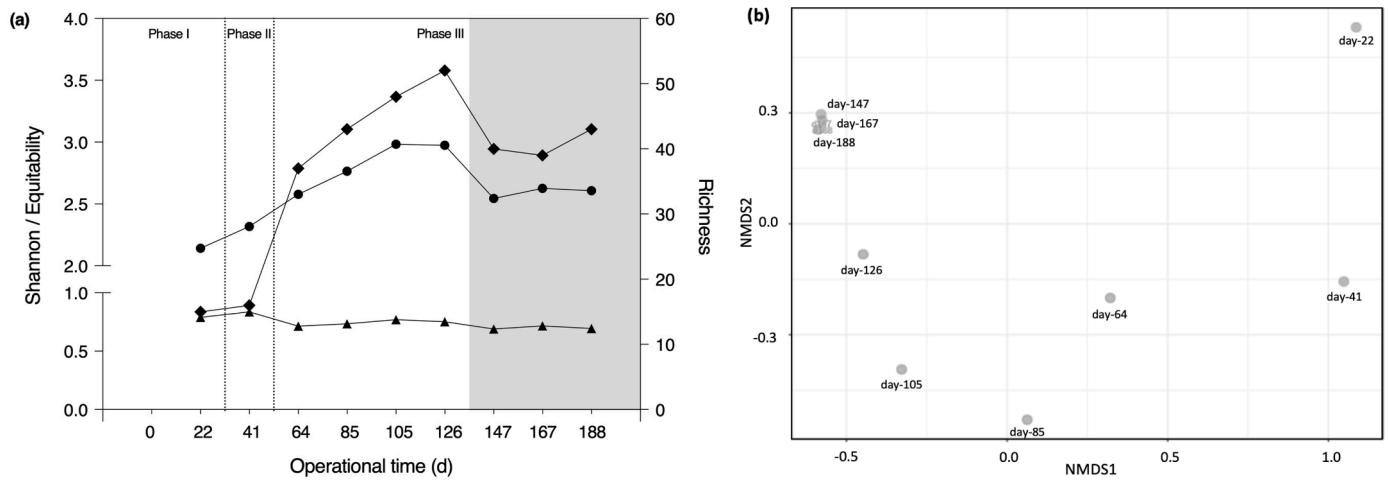

Fig. 6. Alpha and beta diversity analysis and structure of the bacterial community in the reactor biomass. (a) Bacterial community's diversity (Shannon index, ●), equitability (▲), and richness (◆). The gray area indicates the period during which FF loading shocks occurred. (b) NMDS ordination with a stress value of 0.01, using Bray-Curtis distance.

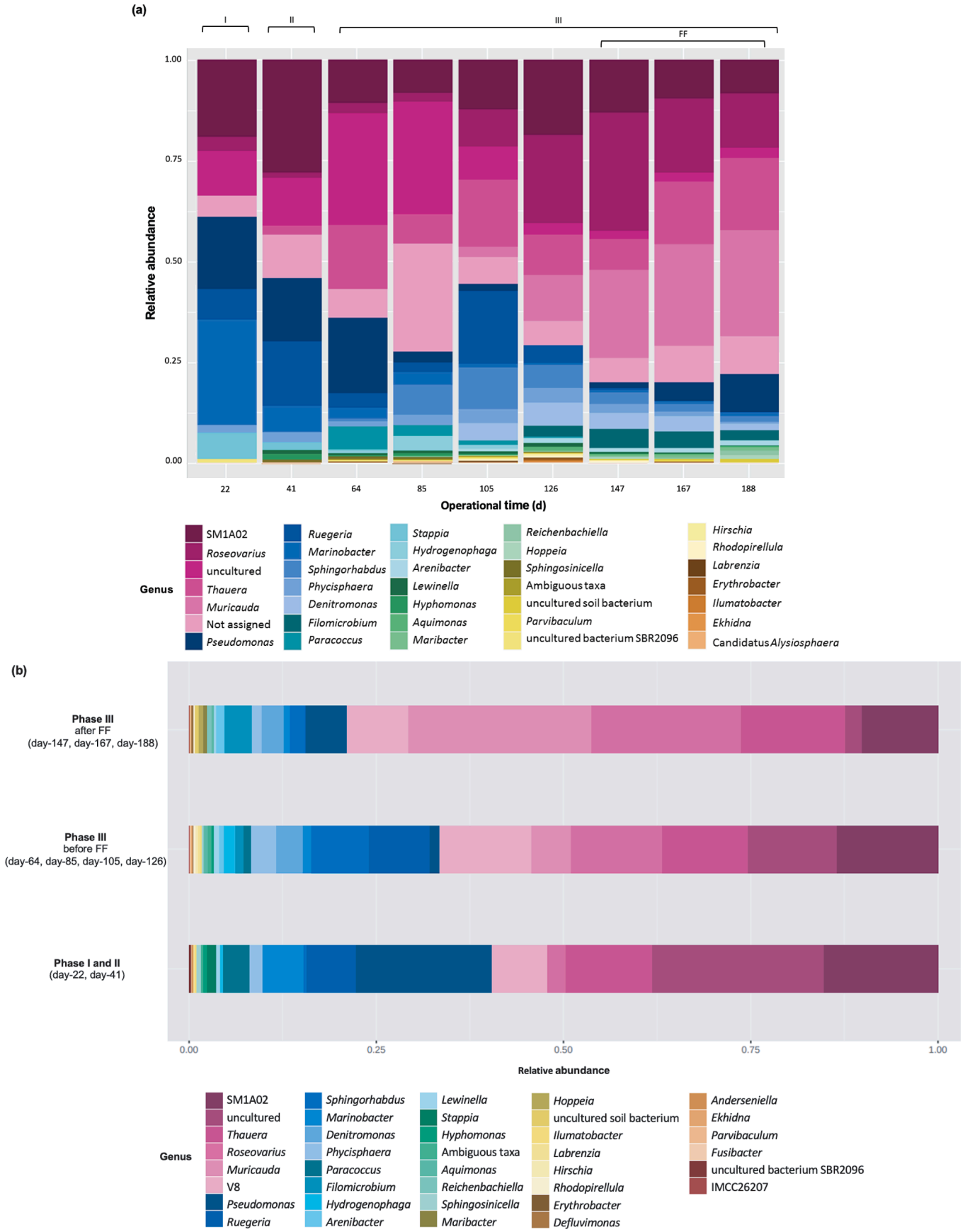

Fig. 7. Bacterial community taxonomic composition at genus level (a) from day-22 to -188; (b) in grouped samples from phase I and II, phase III before FF shock loads, and phase III after FF shock loads.

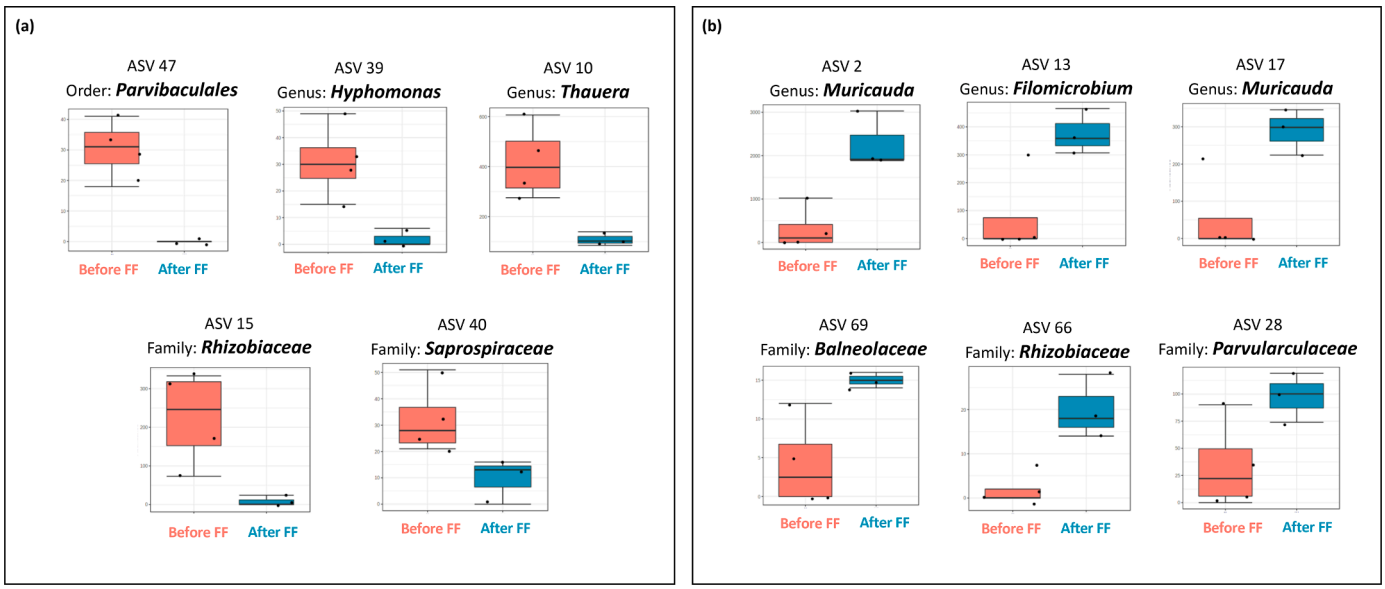

Fig. 8. ASVs with significantly different relative abundances before and after the FF shock loads within phase III (t-test, $p<0.05$): (a) ASVs whose relative abundance decreased after FF shocks; (b) ASVs whose relative abundance increased after FF shocks.

Members of the *Flavobacterium, Brevundimonas*, and *Pseudomonas* genera, and members of the *Sphingomonadaceae* family, found in the bacterial community, have been identified as EPS producers (Subramanian et al., 2010; Verhoef et al., 2002; Weissbrodt et al., 2014). Like certain bacterial strains, microalgae can also produce EPS (Gaignard et al., 2018), but the scarce taxonomic information about the microalgae community found in the present study (mostly high taxonomic levels assigned) makes it difficult to speculate regarding their EPS producing capacity. Interestingly, FF shock loads did not significantly disturb the EPS production. Indeed, some ASVs that proliferated during FF feeding were assigned to EPS producers (Fig. 8a), such as *Muricauda* (Han et al., 2022), while other EPS producers such as *Hyphomonas* (Quintero et al., 1998) and *Saprospiraceae* (Zhu et al., 2022) showed to be susceptible to that stressor (Fig. 8b). Interestingly, some members of the *Rhizobiaceae* family, known EPS producers (Alvarez et al., 2018), have shown to be susceptible to FF while other members of that family proliferated in the same conditions. As reported in previous studies, the microbial community diversity and functional redundancy are key factors for the adaptability and resilience of biological systems under stress factors, allowing for populations susceptible to stressors (e.g., antibiotics) to be replaced by others more adapted to such conditions, enabling the community to cooperate in a synergistic way (Amorim et al., 2018).

A good chemical and microbiological water quality is of utmost importance for the fish growth and survival since their entire life process depends on the quality of the surrounding environment. Therefore, water quality is determinant for the success of aquaculture productions. Table 3 shows the ammonium, nitrite, and nitrate toxicity limits and the dissolved oxygen and pH ideal ranges for brackishwater and marine fish, as well as their concentrations in the reactor effluent when fed with wastewater mimicking coastal aquaculture effluents. Organic carbon and phosphate are not toxic to fish, but high concentrations of these compounds can potentiate the growth of bacteria naturally present in aquaculture pond water, reducing the dissolved oxygen levels, possibly inducing hypoxia, health problems, and mortality in fish (Kim et al., 2013). In the worst-case scenario, it can lead to fish pathogens outbreaks. The high carbon removal efficiency (83 to 100%), even in the presence of FF in the wastewater (Fig. 5a), thus contributes to the high quality of the treated water aiming at recirculation in an aquaculture facility. Contrarily, a low and variable phosphate removal efficiency (<46%) was observed (Fig. 5e), although bacteria assigned to the *Saprospiraceae* family, frequently abundant in enhanced biological phosphorus removal systems (Nielsen et al., 2012), and to *Pseudomonas* genus, known denitrifying polyphosphate-accumulating organisms (He et al., 2018), were detected in the biomass throughout operation. Microalgae can also use phosphorus for growth, as an essential element required for making cellular constituents, or during a stationary phase through the assimilation and storage of polyphosphate (Khanzada, 2020). The well-known Redfield's ratio sets the optimal nutrient ratio required for eukaryotic algae growth as 106:16:1 (C:N:P) (Figler et al., 2021). When the wastewater mimicked an aquaculture effluent (phase III), the C:N:P ratio was of 9.8:1.7:1, which implies a carbon and nitrogen deficiency. Furthermore, environmental factors such as light, osmotic shocks, and nutrient availability have been found to hinder intracellular phosphorus accumulation during microalgae stationary phase (Khanzada, 2020). Thus, the low phosphate removal could have been due to competition between microalgae and bacteria for the available carbon, possibly leading to a low activity of phosphorus removing organisms. Another explanation for the low phosphate removal is linked to the incomplete nitrification process, since nitrite levels as low as 2 mg L^{-1} have been shown to decrease the

Table 3
Ammonium, nitrite, and nitrate toxicity limits, and dissolved oxygen and pH ideal ranges for brackishwater and marine fish, and concentrations detected in the reactor effluent during phase III.

	Reactor effluent (phase III)	Brackishwater and marine fish toxicity limits or ideal ranges	Reference
NH_4^+-N (mg L^{-1})	< 0.09	< 0.3-0.6 [a, b]	Franklin and Edward (2019)
NO_2^- -N (mg L^{-1})	< 3.65	< 38.0 [a]	Costa et al. (2008)
NO_3^- -N (mg L^{-1})	< 7.0	< 10.0 [a]	Camargo et al. (2005)
DO (mg L^{-1}) [c]	> 7.0	> 5.0	Bozorg-Haddad et al. (2021)
pH	8.4-9.2	6.5 – 9.0	Makori et al. (2017)

[a] LC_{50} values
[b] NH_3-N toxicity limit
[c] DO - Dissolved oxygen

polyphosphate-accumulating organisms activity (Saito et al., 2004).

Ammonia is the main nitrogenous waste produced by aquatic animals and is highly toxic to fish (Anusuya et al., 2017). Aqueous ammonia occurs in equilibrium with ammonium, and pH and temperature are major factors influencing their proportions. Since it is very difficult to directly determine the levels of aqueous ammonia, ammonium-nitrogen is quantified, and ammonia-nitrogen concentration is estimated considering the pH and temperature (Franklin and Edward, 2019). Considering the maximum pH and temperature registered during operation (pH 9.2 and 28.7 °C, Fig. S3) and the maximum ammonium-nitrogen effluent concentration (0.09 mg L^{-1}), a maximum ammonia-nitrogen effluent concentration of ca. 0.06 mg L^{-1} was estimated which is below the fish toxicity limits, even for the most sensitive species (Table 3).

Typically, in the presence of multiple nitrogen sources, microalgae often prioritize the ammonium consumption, as this is the most energetically efficient nitrogen source (Perez-Garcia et al., 2011). A slight nitrite accumulation in the effluent was observed (Fig. 5d), probably caused by the simultaneous ammonium oxidation and nitrate reduction into nitrite by microorganisms in the reactor, e.g. members of the genera *Paracoccus, Thauera* and *Denitromonas* likely play a role in the latter (Chen et al., 2020). Nitrate, on the other hand, was degraded by the biomass but with a variable removal efficiency (13-73%) (Fig. 5c). These observations are corroborated by studies by Kaplan et al. (2000) and Huang et al. (2015) who noted that the activity of nitrifying bacteria was significantly reduced when exposed to sunlight, and that nitrite-oxidizing bacteria (NOB) were more sensitive to sunlight than ammonium-oxidizing bacteria, possibly due to the disruption of electron transfer from cytochrome c to nitrite reductase in NOB. Aquatic animals are also sensitive to nitrite and nitrate contents in the water but despite the slight nitrite accumulation and the variable nitrate removal efficiency observed in the present study, the maximum concentrations of both pollutants were maintained below brackishwater and marine fish toxicity limits (Table 3).

Even though the reactor wastewater composition already met the requirements to be recirculated, with ammonia, nitrite, and nitrate concentrations below fish toxicity limits (Table 1 and Table 3), its continuous recirculation without applying any treatment process would lead to the accumulation of pollutants at levels toxic for the fish. Therefore, the biological treatment with the proposed microalgae-based granular sludge could improve even further the water quality, theoretically increasing the number of cycles that water could be recycled. Nevertheless, at this point it is not possible to estimate the number of times that water can be recycled as this study does not take into consideration the accumulation of pollutants in the water due to fish metabolism, that is dependent on fish species, size of the fish tank, and number of fish per tank, and it does not consider the reactor microbial community response to the variable pollution levels on each water recycling cycle. Further research needs to be performed to attest if compounds toxic to fish would build-up or if the microbial community would adapt over time and remove them to a higher extent.

Dissolved oxygen and pH are also important water quality parameters in aquaculture. The pH values in the treated effluent, especially in phase III, were considerably higher than advisable (Table 3). Photosynthetic reactions undertaken by microalgae continuously assimilate CO_2 dissolved in the water, rising the pH to values that may not be adequate for fish rearing. Nevertheless, this can be easily corrected to maintain the pH of the recirculation water within ideal values. Contrarily, the dissolved oxygen levels were within the ideal range for fish growth (Table 3), even exhibiting slightly higher values whenever the FF was present in the wastewater (Fig. S2), probably due to the inhibition of the bacterial activity. The dissolved oxygen level is the first limiting factor in intensive aquaculture systems and one of the main energy consumption components in RAS (Badiola et al., 2018). A biological treatment system such as the one described in the present study represents an attractive solution in RAS, since it reduces the need for oxygenation and, potentially, the aquaculture farm operational costs. On the other hand, energy costs related to LED lights for microalgae survival need to be taken into consideration as well. Further research and life cycle assessment needs to be conducted to confirm lower operational costs and energy savings of this biological treatment system. Nevertheless, the system is promising for decreasing the water needs and dependence of the land-based aquacultures, important issues that this industry is facing due to water scarcity.

Although none of the identified microalgae species belongs to the harmful algae bloom species list, a thorough evaluation of the presence of toxins should be performed to prevent economic losses linked with fish mortality, as well as the transfer of toxins up the food chain.

Microalgae strains such as *Chlorella* sp. *UTEX1602* and *Chlorella* sp. *L38* have been described as able to biodegrade FF at a concentration of 46 mg L^{-1} (97% removal, after 20 days) (Song et al., 2019). Contrarily, *Isochrysis galbana* and *Microcystis flos-aqua* are highly susceptible to FF at 1 mg L^{-1} and 50 μg L^{-1}, respectively, causing biomass growth and chlorophyll production inhibition, as well as oxidative stress in both microalgae species (Wang et al., 2017; Zhang et al., 2020). Evidently, the effect of FF on microalgae growth, viability, and physiology is strain- and dose-dependent. The microalgae-based granular sludge in the present study (Table 2), partially removed FF in the first, third and fourth shock loads most likely due to FF adsorption onto granules. Degradation or biotransformation of the FF seemed to be unlikely to occur within the timeframe of the treatment cycle as fluorine ions, typically released during degradation of fluorinated compounds, were almost absent from the effluent (Fig. S5) and no metabolites were detected by the used HPLC method. Furthermore, FF effluent release on the second shock highlights that adsorption and desorption phenomena are more likely than biotransformation. Several studies have demonstrated the adsorption capacity of granules when subjected to recalcitrant pollutants (Amorim et al., 2017, 2016). The decreasing trend of the removal capacity from the first to the fourth FF shock load also supports adsorption/desorption hypothesis as this is probably linked to saturation of the bonding sites, like what was observed in a previous study (Oliveira et al., 2021).

Further FF removal improvement is required if recirculation is envisaged to prevent its accumulation in the recirculation water and prevent a possible negative impact in the biological treatment microbial community and in the aquaculture fish. For instance, the bioaugmentation of the biological treatment system with FF degrading strains or even chemical and physical methods using for example magnetic biochar as an adsorbent could be integrated in the treatment system or as part of a sequential treatment system and used whenever antibiotics were used in the aquaculture farm (Zhao and Lang, 2018). Nevertheless, further research needs to be conducted to prove the efficiency of such proposed systems.

The reactor inoculum was composed by a non-axenic well-adapted consortium, mainly composed by microalgae. When the 16S rRNA gene was the target region, no sequencing results were obtained for the inoculum (day-0) probably due to the low numbers of bacterial cells in this sample. However, after starting reactor operation a bacterial community has developed. The microalgae and bacterial communities' structure in treatment systems are highly dependent on water quality parameters (nutrient ratios and availability, pH, chemical stressors), environmental factors (temperature, light/darkness cycles), and physiological aspects intrinsic to the microbial community and its symbiotic relations. A dynamic microbial community existed in the granules, whose structure was susceptible and adaptable to the changing operational and environmental reactor conditions (Fig. 7a). The introduction of feeding conditions mimicking coastal aquaculture effluents (phase III), led to the proliferation of known EPS producers and polyhydroxyalkanoates (PHA) storing bacteria, such as *Thauera* (Fall et al., 2022; Świątczak and Cydzik-Kwiatkowska, 2018) and *Paracoccus* (Fall et al., 2022), which may have supported granular stability (Fig. 7b). Interestingly, during the transition from phase II to III, an increase of the relative abundance of a phototrophic bacterial genus, *Roseovarius*

(Fig. 7b) was observed, likely as a response to the lowering carbon content in the wastewater and favorable photosynthetic conditions (Gu and Mitchell, 2006). However, in the same period, a population decrease of the nitrifying and possible anammox genus *SM1A02* occurred, as well as of *Ruegeria* (Fig. 7b), often found in RAS nitrifying filters (Chu et al., 2015; Schreier et al., 2010; Tian et al., 2017; Xie et al., 2021). Considering the nitrification performance, NOB were likely the most affected nitrifying bacteria since nitrite removal was nearly null.

Major bacterial community structural changes and a clear diversity reduction occurred upon FF shock loads (Fig. 6a). The relative abundance of several bacterial ASVs, probably susceptible to this antibiotic, declined considerably, namely ASVs affiliated with genera *Hyphomonas* and *Thauera*, and *Rhizobiaceae, Saprospiraceae*, and *Parvibaculales* families. But the relative abundance of other members of *Thauera* increased after FF shocks (Fig. 8). Members of this genus have shown to have FF resistance genes and members of the *Rhizobiaceae* family were abundant in the intestinal microbiota of fish fed with FF (Gupta et al., 2019; Liu et al., 2021). The introduction of FF also led to the thriving of *Muricauda* and *Filomicrobium* genera, and *Rhizobiaceae* family (Fig. 8), all identified as antibiotic resistant bacteria in literature (Gerzova et al., 2014; Yang et al., 2020; Zhou et al., 2022). Proliferation of *Parvulaculaceae* and of members of the recently established *Balneolaceae* family was also observed (Fig. 8), for which there are no literature reports on antibiotic resistance. Hence, the present study provides evidence that these families might have bacterial strains with FF resistance mechanisms. Microalgae genus *Nitzschia* has also shown to proliferate after FF shocks. The susceptibility of certain bacterial strains to FF could have provided advantageous conditions for this microalgae diatom genus, increasing its capacity to compete for nutrients. In a study performed by Molina-Cárdenas and Sánchez-Saavedra (2017), three *Nitzschia* strains were shown to exert antibacterial activity against pathogenic *Vibrio* species, presumably due to production of inhibitory compounds. It can be hypothesized that a possible synergistic effect could have occurred between the FF shocks and the *Nitzschia* population increase, with both contributing for the bacterial diversity decrease within biomass.

Despite the bacterial diversity reduction and the slight ammonium removal efficiency inhibition (from 100 to >70%) upon FF presence in the wastewater, the removal processes were not disrupted, maintaining the chemical quality of the treated effluent uncompromised. The proposed biological treatment system has the potential to be applied as part of a RAS, promoting water recirculation in a coastal aquaculture farm, and potentially decreasing the costs associated with water oxygenation. As previously stated, the microbial diversity and functional redundancy can play a crucial role in biological systems adaptability, supporting their ability to withstand adverse conditions and environmental stressors.

5. Conclusions

The present study can be regarded as a proof-of-concept for the use of an autochthonous self-granulating microbial consortium in aquaculture effluent bioremediation processes. The main following conclusions were drawn:

- A rapid granulation process occurred (ca. 21 days), supported by increased EPS production, rendering dense granules;
- Microalgae-based granular sludge is a robust and efficient biological treatment system to remove carbon and N species from coastal aquaculture streams, even in periods of FF shock loads, resulting in effluents complying with fish toxicity limits;
- The antibiotic FF was partially removed through sorption, but further improvement of FF removal is needed to prevent its accumulation in recirculation water;
- The study emphasizes the implementation potential of such granular systems in coastal aquaculture facilities, as an integral part of recirculating aquaculture systems, and potentially reducing the farms' oxygenation costs.

Declaration of Competing Interest

The authors declare that they have no known competing financial interests or personal relationships that could have appeared to influence the work reported in this paper.

Data availability

Data will be made available on request.

Acknowledgments

This work was financed by National Funds from FCT - Fundação para a Ciência e a Tecnologia through project GReAT-PTDC/BTA-BTA/29970/2017 (POCI-01-0145-FEDER-029970) and individual grant to Marta Tacão (CEECIND/00977/2020). Authors thank the CBQF, CFE and CESAM scientific collaboration under the FCT projects UIDB/50016/2020, UIDB/04004/2020 and UIDP/50017/2020 + UIDB/50017/2020 + LA/P/0094/2020, respectively.

Supplementary materials

Supplementary material associated with this article can be found, in the online version, at doi:10.1016/j.watres.2023.119733.

References

Ahmed, N., Turchini, G.M., 2021. Recirculating aquaculture systems (RAS): environmental solution and climate change adaptation. J. Clean. Prod. 297, 126604 https://doi.org/10.1016/j.jclepro.2021.126604.

Alvarez, V.M., Jurelevicius, D., Serrato, R.V., Barreto-Bergter, E., Seldin, L., 2018. Chemical characterization and potential application of exopolysaccharides produced by Ensifer adhaerens JHT2 as a bioemulsifier of edible oils. Int. J. Biol. Macromol. 114, 18–25. https://doi.org/10.1016/j.ijbiomac.2018.03.063.

Amaral-Zettler, L.A., McCliment, E.A., Ducklow, H.W., Huse, S.M., 2009. A method for studying protistan diversity using massively parallel sequencing of V9 hypervariable regions of small-subunit ribosomal RNA Genes. PLoS One 4, 1–9. https://doi.org/10.1371/journal.pone.0006372.

Amorim, C.L., Alves, M., Castro, P.M.L., Henriques, I., 2018. Bacterial community dynamics within an aerobic granular sludge reactor treating wastewater loaded with pharmaceuticals. Ecotoxicol. Environ. Saf. 147, 905–912. https://doi.org/10.1016/j.ecoenv.2017.09.060.

Amorim, C.L., Moreira, I.S., Duque, A.F., van Loosdrecht, M.C., Castro, P.M., 2017. Aerobic granular sludge: treatment of wastewaters containing toxic compounds, in: Technologies for the Treatment and Recovery of Nutrients from Industrial Wastewater. pp. 231–363. doi:10.4018/978-1-5225-1037-6.ch009.

Amorim, C.L., Moreira, I.S., Ribeiro, A.R., Santos, L.H.M.L.M., Delerue-Matos, C., Tiritan, M.E., Castro, P.M.L., 2016. Treatment of a simulated wastewater amended with a chiral pharmaceuticals mixture by an aerobic granular sludge sequencing batch reactor. Int. Biodeterior Biodegradation 115, 277–285. https://doi.org/10.1016/j.ibiod.2016.09.009.

An, W., Guo, F., Song, Y., Gao, N., Bai, S., Dai, J., Wei, H., Zhang, L., Yu, D., Xia, M., Yu, Y., Qi, M., Tian, C., Chen, H., Wu, Z., Zhang, T., Qiu, D., 2016. Comparative genomics analyses on EPS biosynthesis genes required for floc formation of Zoogloea resiniphila and other activated sludge bacteria. Water Res. 102, 494–504. https://doi.org/10.1016/j.watres.2016.06.058.

Anderson, M., Gorley, R.N., Clarke, K.R., 2008. PERMANOVA+ for PRIMER: Guide to Software and Statistical Methods.

Ansari, F.A., Gupta, S.K., Bux, F, 2019. Application of Microalgae in Wastewater Treatment, in: Gupta, S., Bux, F. (Eds.), Application of Microalgae in Wastewater Treatment. pp. 69–83. 10.1007/978-3-030-13909-4_4.

Ansari, F.A., Singh, P., Guldhe, A., Bux, F., 2017. Microalgal cultivation using aquaculture wastewater: Integrated biomass generation and nutrient remediation. Algal Res. 21, 169–177. https://doi.org/10.1016/j.algal.2016.11.015.

Anusuya, P.D., Padmavathy, P., Aanand, S., Aruljothi, K., 2017. Review on water quality parameters in freshwater cage fish culture. Int. J. Appl. Res. 3, 114–120.

APHA, 1998. Standard Methods for the Examination of Water and Wastewater. American Public Health Association.

Badiola, M., Basurko, O.C., Piedrahita, R., Hundley, P., Mendiola, D., 2018. Energy use in Recirculating Aquaculture Systems (RAS): a review. Aquac. Eng. 81, 57–70. https://doi.org/10.1016/j.aquaeng.2018.03.003.

Bodenhausen, N., Horton, M.W., Bergelson, J., 2013. Bacterial communities associated with the leaves and the roots of arabidopsis thaliana. PLoS One 8, e56329. https://doi.org/10.1371/journal.pone.0056329.

Bolyen, E., Rideout, J.R., Dillon, M.R., et al., 2019. Reproducible, interactive, scalable and extensible microbiome data science using QIIME 2. Nat. Biotechnol. 37, 852–857. https://doi.org/10.1038/s41587-019-0209-9.

Bozorg-Haddad, O., Delpasand, M., Loáicig, H.A., 2021. Water quality, hygiene, and health. In: Bozorg-Haddad, O. (Ed.), Economical, Political, and Social Issues in Water Resources. Elsevier Inc., pp. 217–256

Bradley, I.M., Pinto, A.J., Guest, J.S., 2016. Gene-Specific primers for improved characterization of mixed phototrophic communities. Appl. Environ. Microbiol. 82, 5878–5891. https://doi.org/10.1128/AEM.01630-16.Editor.

Bulgarelli, D., Rott, M., Schlaeppi, K., Ver Loren van Themaat, E., Ahmadinejad, N., Assenza, F., Rauf, P., Huettel, B., Reinhardt, R., Schmelzer, E., Peplies, J., Gloeckner, F.O., Amann, R., Eickhorst, T., Schulze-Lefert, P., 2012. Revealing structure and assembly cues for Arabidopsis root-inhabiting bacterial microbiota. Nature 488, 91–95. https://doi.org/10.1038/nature11336.

Callahan, B.J., McMurdie, P.J., Rosen, M.J., Han, A.W., Johnson, A.J.A., Holmes, S.P., 2016. DADA2: high-resolution sample inference from Illumina amplicon data. Nat. Methods 13, 581–583. https://doi.org/10.1038/nmeth.3869.

Camargo, J.A., Alonso, A., Salamanca, A., 2005. Nitrate toxicity to aquatic animals: a review with new data for freshwater invertebrates. Chemosphere 58, 1255–1267. https://doi.org/10.1016/j.chemosphere.2004.10.044.

Chen, S., Li, S., Huang, T., Yang, S., Liu, K., Ma, B., Shi, Y., Miao, Y., 2020. Nitrate reduction by Paracoccus thiophilus strain LSL 251 under aerobic condition: Performance and intracellular central carbon flux pathways. Bioresour. Technol. 308, 123301 https://doi.org/10.1016/j.biortech.2020.123301.

Chu, Z., Wang, K., Li, X., Zhu, M., Yang, L., Zhang, J., 2015. Microbial characterization of aggregates within a one-stage nitritation-anammox system using high-throughput amplicon sequencing. Chem. Eng. J. 262, 41–48. https://doi.org/10.1016/j.cej.2014.09.067.

Costa, L.D.F., Miranda-Filho, K.C., Severo, M.P., Sampaio, L.A., 2008. Tolerance of juvenile pompano Trachinotus marginatus to acute ammonia and nitrite exposure at different salinity levels. Aquaculture 285, 270–272. https://doi.org/10.1016/j.aquaculture.2008.08.017.

Dauda, A.B., Ajadi, A., Tola-Fabunmi, A.S., Akinwole, A.O., 2019. Waste production in aquaculture: sources, components and managements in different culture systems. Aquac Fish 4, 81–88. https://doi.org/10.1016/j.aaf.2018.10.002.

Dhariwal, A., Chong, J., Habib, S., King, I.L., Agellon, L.B., Xia, J., 2017. MicrobiomeAnalyst: a web-based tool for comprehensive statistical, visual and meta-analysis of microbiome data. Nucleic. Acids. Res. 45, W180–W188. https://doi.org/10.1093/nar/gkx295.

Dubois, M., Gilles, K.A., Hamilton, J.K., Rebers, P.A., Smith, F., 1956. Colorimetric method for determination of sugars and related substances. Anal. Chem. 28, 350–356. https://doi.org/10.1021/ac60111a017.

Duque, A.F., Bessa, V.S., Carvalho, M.F., de Kreuk, M.K., van Loosdrecht, M.C.M., Castro, P.M.L., 2011. 2-Fluorophenol degradation by aerobic granular sludge in a sequencing batch reactor. Water Res. 45, 6745–6752. https://doi.org/10.1016/j.watres.2011.10.033.

Ebeling, J.M., Timmons, M.B., 2012. Recirculating aquaculture systems. In: Tidwell, J. (Ed.), Aquaculture Production Systems. John Wiley & Sons, Inc, pp. 245–277. https://doi.org/10.1002/9781118250105.ch11.

Fall, C., Barrón-Hernández, L.M., Gonzaga-Galeana, V.E., Olguín, M.T., 2022. Ordinary heterotrophic organisms with aerobic storage capacity provide stable aerobic granular sludge for C and N removal. J. Environ. Manage. 308 https://doi.org/10.1016/j.jenvman.2022.114662.

Fan, S., Ji, B., Abu Hasan, H., Fan, J., Guo, S., Wang, J., Yuan, J., 2021. Microalgal–bacterial granular sludge process for non-aerated aquaculture wastewater treatment. Bioprocess. Biosyst. Eng. 44, 1733–1739. https://doi.org/10.1007/s00449-021-02556-0.

FAO, 2022. The State of World Fisheries and Aquaculture 2022. Towards Blue Transformation. Rome, FAO. 10.4060/cc0461en.

Fernando, J.S, Gressler, LT., 2021. Chapter 3 - Antimicrobial agents. In: Kibenge, F.S.B., Baldisserotto, B., Chong, R.S.-M. (Eds.), Aquaculture Pharmacology. Academic Press, pp. 131–168.

Figler, A., Márton, K., B-Béres, V., Bácsi, I., 2021. Effects of nutrient content and nitrogen to phosphorous ratio on the growth, nutrient removal and desalination properties of the green alga coelastrum morus on a laboratory scale. Energies (Basel) 14, 2112. https://doi.org/10.3390/en14082112.

Franklin, D.A., Edward, L.L., 2019. Ammonia toxicity and adaptive response in marine fishes - A review. Indian J. Geo-Marine Sci. 48, 273–279.

Gaignard, C., Laroche, C., Pierre, G., Dubessay, P., Delattre, C., Gardarin, C., Gourvil, P., Probert, I., Dubuffet, A., Michaud, P., Shniukova, E.I., Zolotareva, E.K., Aslam, S.N., Strauss, J., Thomas, D.N., Mock, T., Underwood, G.J.C., Babiak, W., Krzemińska, I., 2018. Extracellular polymeric substances (EPS) as microalgal bioproducts: A review of factors affecting EPS synthesis and application in flocculation processes. Energies (Basel) 17, 1237–1251. https://doi.org/10.3390/en14134007.

Gao, F., Li, Z., Chang, Q., Gao, M., She, Z., Wu, J., Jin, C., Zheng, D., Guo, L., Zhao, Y., Wang, S., 2018. Effect of florfenicol on performance and microbial community of a sequencing batch biofilm reactor treating mariculture wastewater. Environ. Technol. 39, 363–372. https://doi.org/10.1080/09593330.2017.1301567.

Gerzova, L., Videnska, P., Faldynova, M., Sedlar, K., Provaznik, I., Cizek, A., Rychlik, I., 2014. Characterization of microbiota composition and presence of selected antibiotic resistance genes in carriage water of ornamental fish. PLoS One 9, e103865. https://doi.org/10.1371/journal.pone.0103865.

Gu, J., Mitchell, R., Dworkin, M., Falkow, S., Rosenberg, E., Schleifer, KH., 2006. Aerobic Phototrophic Proteobacteria. In: Stackebrandt, E. (Ed.), The Prokaryotes. Springer, New York, NY, pp. 3–893. https://doi.org/10.1007/0-387-30745-1_23.

Guldhe, A., Ansari, F.A., Singh, P., Bux, F., 2017. Heterotrophic cultivation of microalgae using aquaculture wastewater: A biorefinery concept for biomass production and nutrient remediation. Ecol. Eng. 99, 47–53. https://doi.org/10.1016/j.ecoleng.2016.11.013.

Guo, Z., Liu, Y., Guo, H., Yan, S., Mu, J., 2013. Microalgae cultivation using an aquaculture wastewater as growth medium for biomass and biofuel production. J. Environ. Sci. 25, S85–S88. https://doi.org/10.1016/S1001-0742(14)60632-X.

Gupta, S., Fernandes, J., Kiron, V., 2019. Antibiotic-induced perturbations are manifested in the dominant intestinal bacterial phyla of Atlantic salmon. Microorganisms 7, 233–253. https://doi.org/10.3390/microorganisms7080233.

Han, F., Zhang, M., Liu, Z., Han, Y., Li, Q., Zhou, W., 2022. Enhancing robustness of halophilic aerobic granule sludge by granular activated carbon at decreasing temperature. Chemosphere 292, 133507. https://doi.org/10.1016/j.chemosphere.2021.133507.

He, Q., Song, Q., Zhang, S., Zhang, W., Wang, H., 2018. Simultaneous nitrification, denitrification and phosphorus removal in an aerobic granular sequencing batch reactor with mixed carbon sources: reactor performance, extracellular polymeric substances and microbial successions. Chem. Eng. J. 331, 841–849. https://doi.org/10.1016/j.cej.2017.09.060.

Henriques, M., Silva, a, Rocha, J., 2007. Extraction and quantification of pigments from a marine microalga : a simple and reproducible method. Communicating Current Research and Educational Topics and Trends in Applied Microbiology 586–593.

Huang, W., Li, B., Zhang, C., Zhang, Z., Lei, Z., Lu, B., Zhou, B., 2015. Effect of algae growth on aerobic granulation and nutrients removal from synthetic wastewater by using sequencing batch reactors. Bioresour. Technol. 179, 187–192. https://doi.org/10.1016/j.biortech.2014.12.024.

Jangaran Nejad, A., Peyghan, R., Varzi, H.N., Shahriyari, A., Jangaran, A., Phd, N., 2017. Florfenicol pharmacokinetics following intravenous and oral administrations and its elimination after oral and bath administrations in common carp (Cyprinus carpio). ARTICLE Veterinary Research Forum.

Kaplan, D., Wilhelm, R., Abeliovich, A., 2000. Interdependent environmental factors controlling nitrification in waters. Water Sci. Technol. 42, 167–172. https://doi.org/10.2166/wst.2000.0309.

Khanzada, Z.T., 2020. Phosphorus removal from landfill leachate by microalgae. Biotechnol. Rep. 25, e00419. https://doi.org/10.1016/j.btre.2020.e00419.

Khatoon, H., Banerjee, S., Syakir Syahiran, M., Mat Noordin, N.B., Munafi Ambok Bolong, A., Endut, A., 2016. Re-use of aquaculture wastewater in cultivating microalgae as live feed for aquaculture organisms. Desalination Water Treat. 57, 29295–29302. https://doi.org/10.1080/19443994.2016.1156030.

Kim, E., Yoo, S., Ro, H., Han, H., Baek, Y., Eom, I., Kim, H., Kim, P., Choi, K., 2013. Aquatic toxicity assessment of phosphate compounds. Environ. Health Toxicity 28, 1–7. https://doi.org/10.5620/eht.2013.28.e2013002.

Lee, Y.J., Lei, Z., 2019. Microalgal-bacterial aggregates for wastewater treatment: a mini-review. Bioresour. Technol. Rep. 8, 100199 https://doi.org/10.1016/j.biteb.2019.100199.

Li, H., Chen, S., Liao, K., Lu, Q., Zhou, W., 2021. Microalgae biotechnology as a promising pathway to ecofriendly aquaculture: a state-of-the-art review. J. Chem. Technol. Biotechnol. 96, 837–852. https://doi.org/10.1002/jctb.6624.

Li, K., Liu, Q., Fang, F., Luo, R., Lu, Q., Zhou, W., Huo, S., Cheng, P., Liu, J., Addy, M., Chen, P., Chen, D., Ruan, R., 2019. Microalgae-based wastewater treatment for nutrients recovery: A review. Bioresour. Technol. 291, 121934 https://doi.org/10.1016/j.biortech.2019.121934.

Liu, H., Ding, Y., Tang, H., Du, Y., Zhang, D., Tang, Y., Liu, C., 2021. Electrocatalytic deep dehalogenation of florfenicol using Fe-doped CoP nanotubes array for blocking resistance gene expression and microbial inhibition during biochemical treatment. Water Res. 201, 117361 https://doi.org/10.1016/j.watres.2021.117361.

Liu, Y., Lv, J., Feng, J., Liu, Q., Nan, F., Xie, S., 2019. Treatment of real aquaculture wastewater from a fishery utilizing phytoremediation with microalgae. J. Chem. Technol. Biotechnol. 94, 900–910. https://doi.org/10.1002/jctb.5837.

Lowry, O.H., Rosebrough, N.J., Farr, A.L., Randall, R.J., 1951. Protein measurement with the folin phenol reagent. J. Biol. Chem. 193, 265–275. https://doi.org/10.1016/S0021-9258(19)52451-6.

Makori, A.J., Abuom, P.O., Kapiyo, R., Anyona, D.N., Dida, G.O., 2017. Effects of water physico-chemical parameters on tilapia (Oreochromis niloticus) growth in earthen ponds in Teso North Sub-County, Busia County. Fish Aquatic Sci. 20, 1–10. https://doi.org/10.1186/s41240-017-0075-7.

Molina-Cárdenas, C.A., Sánchez-Saavedra, M.P., 2017. Inhibitory effect of benthic diatom species on three aquaculture pathogenic vibrios. Algal Res. 27, 131–139. https://doi.org/10.1016/j.algal.2017.09.004.

Nielsen, P.H., Saunders, A.M., Hansen, A.A., Larsen, P., Nielsen, J.L., 2012. Microbial communities involved in enhanced biological phosphorus removal from wastewater-a model system in environmental biotechnology. Curr. Opin. Biotechnol. 23, 452–459. https://doi.org/10.1016/j.copbio.2011.11.027.

Oliveira, A.S., Amorim, C.L., Mesquita, D.P., Ferreira, E.C., van Loosdrecht, M., Castro, P.M.L., 2021. Increased extracellular polymeric substances production contributes for the robustness of aerobic granular sludge during long-term intermittent exposure to 2-fluorophenol in saline wastewater. J. Water Process Eng. 40, 101977 https://doi.org/10.1016/j. jwpe. 2021.101977.

Oliveira, A.S., Amorim, C.L., Ramos, M.A., Mesquita, D.P., Inocêncio, P., Ferreira, E.C., Loosdrecht, M., Castro, P.M.L., 2020. Variability in the composition of extracellular polymeric substances from a full-scale aerobic granular sludge reactor treating urban wastewater. J. Environ. Chem. Eng. 8, 104156 https://doi.org/10.1016/j.jece.2020.104156.

Perez-Garcia, O., Escalante, F.M.E., de-Bashan, L.E., Bashan, Y., 2011. Heterotrophic cultures of microalgae: Metabolism and potential products. Water Res. 45, 11–36. https://doi.org/10.1016/j.watres.2010.08.037.

Quast, C., Pruesse, E., Yilmaz, P., Gerken, J., Schweer, T., Yarza, P., Peplies, J., Glöckner, F.O., 2013. The SILVA ribosomal RNA gene database project: Improved data processing and web-based tools. Nucleic. Acids. Res. 41, 590–596. https://doi.org/10.1093/nar/gks1219.

Quintero, E.J., Busch, K., Weiner, R.M., 1998. Spatial and temporal deposition of adhesive extracellular polysaccharide capsule and fimbriae by Hyphomonas strain MHS-3. Appl. Environ. Microbiol. 64, 1246–1255. https://doi.org/10.1128/aem.64.4.1246-1255.1998.

Rajitha, K., Sarvajith, M., Venugopalan, V.P., Nancharaiah, Y.V., 2020. Development and performance of halophilic microalgae-colonized aerobic granular sludge for treating seawater-based wastewater. Bioresour. Technol. Rep. 11, 100432 https://doi.org/10.1016/j.biteb.2020.100432.

Reverter, M., Sarter, S., Caruso, D., Avarre, J.C., Combe, M., Pepey, E., Pouyaud, L., Vega-Heredía, S., de Verdal, H., Gozlan, R.E., 2020. Aquaculture at the crossroads of global warming and antimicrobial resistance. Nat. Commun. 11, 1–8. https://doi.org/10.1038/s41467-020-15735-6.

Saito, T., Brdjanovic, D., Van Loosdrecht, M.C.M., 2004. Effect of nitrite on phosphate uptake by phosphate accumulating organisms. Water Res. 38, 3760–3768. https://doi.org/10.1016/j.watres.2004.05.023.

Santorio, S., Couto, A.T., Amorim, C.L., Val del Rio, A., Arregui, L., Mosquera-Corral, A., Castro, P.M.L., 2021. Sequencing versus continuous granular sludge reactor for the treatment of freshwater aquaculture effluents. Water Res. 201, 117293 https://doi.org/10.1016/j.watres.2021.117293.

Santorio, S., Val del Río, A., Amorim, C.L., Couto, A.T., Arregui, L., Castro, P.M.L., Mosquera-Corral, A., 2022. Are Pn-Anammox and microalgae-bacterial biomass continuous-flow granular reactors feasible oxygen saving alternatives when facing extremely low-strength freshwater aquaculture streams? SSRN Electronic J. 4092258 https://doi.org/10.2139/ssrn.4092258.

Schreier, H.J., Mirzoyan, N., Saito, K., 2010. Microbial diversity of biological filters in recirculating aquaculture systems. Curr. Opin. Biotechnol. 21, 318–325. https://doi.org/10.1016/j.copbio.2010.03.011.

Song, C., Wei, Y., Qiu, Y., Qi, Y., Li, Y., Kitamura, Y., 2019. Biodegradability and mechanism of florfenicol via Chlorella sp. UTEX1602 and L38: Experimental study. Bioresour. Technol. 272, 529–534. https://doi.org/10.1016/j.biortech.2018.10.080.

Subramanian, S.B., Yan, S., Tyagi, R.D., Surampalli, R.Y., 2010. Extracellular polymeric substances (EPS) producing bacterial strains of municipal wastewater sludge: Isolation, molecular identification, EPS characterization and performance for sludge settling and dewatering. Water Res. 44, 2253–2266. https://doi.org/10.1016/j.watres.2009.12.046.

Sumanta, N., Haque, C.I., Nishika, J., Suprakash, R., 2014. Spectrophotometric analysis of chlorophylls and carotenoids from commonly grown fern species by using various extracting solvents. Res. J. Chem. Sci. 4, 2231–2606. https://doi.org/10.1055/s-0033-1340072.

Świątczak, P., Cydzik-Kwiatkowska, A., 2018. Treatment of ammonium-rich digestate from methane fermentation using aerobic granular Sludge. Water Air Soil Pollut. 229, 229–247. https://doi.org/10.1007/s11270-018-3887-x.

Thomsen, E., Herbeck, L.S., Jennerjahn, T.C., 2020. The end of resilience: Surpassed nitrogen thresholds in coastal waters led to severe seagrass loss after decades of exposure to aquaculture effluents: Long-term aquaculture effluents exposure causes seagrass loss. Mar. Environ. Res. 160, 104986 https://doi.org/10.1016/j.marenvres.2020.104986.

Tian, S., Tian, Z., Yang, H., Yang, M., Zhang, Y., 2017. Detection of viable bacteria during sludge ozonation by the combination of ATP assay with PMA-miseq sequencing. Water (Basel) 9, 166–177. https://doi.org/10.3390/w9030166.

Verhoef, R., De Waard, P., Schols, H.A., Rättö, M., Siika-Aho, M., Voragen, A.G.J., 2002. Structural elucidation of the EPS of slime producing Brevundimonas vesicularis sp. isolated from a paper machine. Carbohydr. Res. 337, 1821–1831. https://doi.org/10.1016/S0008-6215(02)00280-X.

Vo, H.N.P., Ngo, H.H., Guo, W., Chang, S.W., Nguyen, D.D., Chen, Z., Wang, X.C., Chen, R., Zhang, X., 2020. Microalgae for saline wastewater treatment: a critical review. Crit. Rev. Environ. Sci. Technol. 50, 1224–1265. https://doi.org/10.1080/10643389.2019.1656510.

Wang, M., Zhang, Y., Guo, P., 2017. Effect of florfenicol and thiamphenicol exposure on the photosynthesis and antioxidant system of Microcystis flos-aquae. Aquatic Toxicol. 186, 67–76. https://doi.org/10.1016/j.aquatox.2017.02.022.

Wang, Q., Shen, Q., Wang, J., Zhao, J., Zhang, Z., Lei, Z., Yuan, T., Shimizu, K., Liu, Y., Lee, D.J., 2022. Insight into the rapid biogranulation for suspended single-cell microalgae harvesting in wastewater treatment systems: Focus on the role of extracellular polymeric substances. Chem. Eng. J. 430, 132631 https://doi.org/10.1016/j.cej.2021.132631.

Weissbrodt, D.G., Shani, N., Holliger, C., 2014. Linking bacterial population dynamics and nutrient removal in the granular sludge biofilm ecosystem engineered for wastewater treatment. FEMS Microbiol. Ecol. 88, 579–595. https://doi.org/10.1111/1574-6941.12326.

Xiao, R., Wei, Y., An, D., Li, D., Ta, X., Wu, Y., Ren, Q., 2019. A review on the research status and development trend of equipment in water treatment processes of recirculating aquaculture systems. Rev. Aquac. 11, 863–895. https://doi.org/10.1111/raq.12270.

Xie, F., Zhao, B., Cui, Y., Ma, X., Zhang, X., Yue, X., 2021. Reutilize tire in microbial fuel cell for enhancing the nitrogen removal of the anammox process coupled with iron-carbon micro-electrolysis. Front. Environ. Sci. Eng. 15, 121–132. https://doi.org/10.1007/s11783-021-1409-3.

Yang, X., Song, X., Hallerman, E., Huang, Z., 2020. Microbial community structure and nitrogen removal responses of an aerobic denitrification biofilm system exposed to tetracycline. Aquaculture 529, 735665. https://doi.org/10.1016/j.aquaculture.2020.735665.

Zhang, Y., Zhang, X., Guo, R., Zhang, Q., Cao, X., Suranjana, M., Liu, Y., 2020. Effects of florfenicol on growth, photosynthesis and antioxidant system of the non-target organism Isochrysis galbana. Comp. Biochem. Physiol. Part - C: Toxicol. 233, 108764 https://doi.org/10.1016/j.cbpc.2020.108764.

Zhao, H., Lang, Y., 2018. Adsorption behaviors and mechanisms of florfenicol by magnetic functionalized biochar and reed biochar. J. Taiwan Inst. Chem. Eng. 88, 152–160. https://doi.org/10.1016/j.jtice.2018.03.049.

Zhou, Z., Song, Z., Gu, J., Wang, X., Hu, T., Guo, H., Xie, J., Lei, L., Ding, Q., Jiang, H., Xu, L., 2022. Dynamics and key drivers of antibiotic resistance genes during aerobic composting amended with plant-derived and animal manure-derived biochars. Bioresour. Technol. 355, 127236 https://doi.org/10.1016/j.biortech.2022.127236.

Zhu, X., Lee, L.W., Song, G., Zhang, X., Gao, Y., Yang, G., Luo, S., Huang, X., 2022. Deciphering mono/multivalent draw solute-induced microbial ecology and membrane fouling in anaerobic osmotic membrane bioreactor. Water Res. 209, 117869 https://doi.org/10.1016/j.watres.2021.117869.

Zong, H., Ma, D., Wang, J., Hu, J., 2010. Research on florfenicol residue in coastal area of dalian (Northern China) and analysis of functional diversity of the microbial community in marine sediment. Bull. Environ. Contam. Toxicol. 84, 245–249. https://doi.org/10.1007/s00128-009-9923-1.